Proceedings World Geothermal Congress 2015
Melbourne, Australia, 19-25 April 2015

Remote Sensing and GPR Studies of Faults Bounding the Irosin Caldera, Luzon, Philippines

Eden G. Baliatan-Sernadilla[1 2] and Alfredo Mahar F. A. Lagmay[2]

[1]Energy Development Corporation, 38F One Corporate Centre, Julia Vargas cor Meralco Ave, Ortigas Center, Pasig City Philippines

baliatan.eg@energy.com.ph

[2]National Institute of Geological Sciences, University of the Philippines, Diliman, Quezon City 1101, Philippines

Keywords: Irosin caldera, Ground Penetrating Radar, Shaded Relief Images, Aspect Maps.

ABSTRACT

The Irosin caldera, located at the southernmost tip of the Bicol Volcanic Arc, Luzon, Philippines was investigated for regional tectonic structures through remote-sensing and Ground Penetrating Radar (GPR). Four shaded relief images and two slope aspect maps were derived from high resolution Synthetic Aperture Radar (SAR) Digital Surface Model (DSM) and used to carry out lineament analysis of the area. A network of WNW-SE, NNW-SSE and NE-SW-trending structures, particularly the large-scale ones, were consistently delineated in all the generated topographic models. The most prominent lineaments identified are the WNW-SE-trending linear features that border the northern and southern rim of the Irosin caldera.

A GPR survey was carried out by common offset method across the southern lineament using a 100 Mhz antenna to locate and verify its continuity. The GPR data provided relatively high-resolution radargrams of the upper 10m of the subsurface. These profiles revealed dense arrays of fractures and faults, with various angles of dip, spatial orientation and depths, which coincide with the projected location of the southern lineament. The results of the survey proved that the southern caldera fault is continuous. The central segment of the southern lineament is most likely overlain by thick volcanic deposits from the recent volcanic eruption of the nearby Bulusan Volcano, making them difficult to identify on the topographic models. Some structures have also been identified outside of the projected location of the fault, and may likely be some of the numerous fractures and ring faults that are commonly expected along the periphery of calderas.

1. INTRODUCTION

Volcanoes and volcanism are intimately related to the regional tectonic setting (Pasquare and Tibaldi, 2003). In particular, regional tectonic structures, such as faults and fractures, offer pathways of least resistance for magma to ascend and erupt (Acocella et al., 1999). Because of the influence of tectonic structures, elongate and polygonal calderas form instead of the normal circular or semicircular shapes. Examples of these include the elongate calderas of Toba and Ranau (Bellier and Sébrier, 1994) and the polygonal shape of Tondano (Lecuyer et al., 1997). Analog experiments of calderas formed in active pre-existing tectonic structures demonstrated that elliptical or elongate calderas may form above circular magma chambers when subjected to regional stress during its formation (Holohan et al., 2005). Magma chamber elongation as a result of deep-rooted pre-existing strike-slip faults also lead to the formation of elongate calderas (Holohan et al., 2008).

Initial observations of the planform of the Irosin caldera show a polygonal-shaped depression with its northern and southern rim bounded by WNW-ESE-trending linear features. On the basis of Sanderson and Marchini's (1984) transtensional strain model, Lagmay et al. (2005) suggested that the Bicol Peninsula is situated within a releasing bend of the Philippine Fault and movement along the central segment would generate NW-SE-trending transtensional fault splays. Within the study area, WNW-SE alignment of volcanoes and volcanic domes are evident and suggest volcanism guided by basement structures consistent with the regional trend of tectonic structures in the Bicol Peninsula (Delfin, 1991).

Because tectonic deformation alters the relief of a region and may control topography such as the distribution and arrangement of volcanoes, river systems and ridges, morphotectonic analysis was conducted on the study area. The topographic models of the Bulusan Volcanic Complex were analyzed for linear features such as valleys, rivers and ridges, offset structures, and aligned volcanic centers that may indicate the type of deformation that occurs in the area. This technique is particularly useful on active volcanoes in tropical areas where eruption deposits, dense vegetation cover, weathering and rapid erosion affects the preservation of structures.

The interpretation of shaded relief and slope aspect maps showed that they are effective tools in locating target sites that warrant more detailed structural investigation. In particular, large-scale linear features found to border the southern rim of the Irosin caldera were verified in the field using Ground Penetrating Radar (GPR). This study utilized GPR to locate and verify the continuity of the central segment of the west northwest-trending lineament that bounds the southern rim of the Irosin Caldera (Figure 2). As the structure is located within the caldera itself, surface manifestations are difficult to identify due to the thick volcanic fill. These deposits, known collectively as the Irosin Ignimbrite, are largely loosely consolidated, therefore structures that propagate through them are poorly preserved. Furthermore, recent eruptive products of the active Bulusan Volcano make it more challenging to locate tectonic structures. Because of these limitations, field structural mapping is best aided by geophysical methods which image the subsurface.

2. STUDY AREA

Located within Luzon Island at the southernmost tip of the Bicol Volcanic Arc is the Bulusan Volcanic Complex, which consists of an active volcano, an 11-km diameter caldera, and several eroded craters and volcanic cones (Figure 1). The volcanic activity

within the complex can be dated as far back as 2.14 Ma with the formation of high-K volcanic suite represented by the Gate volcanics (Delfin, 1991; Delfin et al., 1993)

The younger Pliocene-Holocene volcanic suite has been subdivided into three major stages of volcanism, the precaldera, caldera and postcaldera stages, based on the synthesis of stratigraphic, geomorphic, radiometric, petrologic and geochemical data.Construction of medium-K basaltic andesite and andesite stratovolcanoes along probable regional fractures marked the precaldera stage, which began at least 1.1 Ma. This was followed by a major eruption of rhyolitic pumice-flows about 41 ka (Mirabueno et al., 2007) that led to the formation of the 11 km-wide Irosin caldera. Subsequent to the formation of the caldera, resurgent activity resulted in the development of randomly distributed domes such as Jormajam and Talatak and the formation of Bulusan Volcano within the caldera (Delfin, 1991)

The Irosin Caldera bounds the towns of Irosin, Bulusan and Juban. It is named after the town that has greatest map coverage of its planform. The calderagenic eruption that formed this volcanic depression deposited the Irosin Ignimbrite over an area of at least 400 sq. km, with a total volume estimated to be about 60 cu. km (Delfin, 1991). The Irosin Ignimbrite has a thickness of at least 20 m in flat-lying areas. An estimate of the minimum amount of subsidence along the caldera walls, based on the topographic relief between the rim and caldera floor, is about 100 m in the west, 150 m in the southwest and 560 m in the southeast (Delfin, 1991). The caldera rim is absent in the north due to the presence of Bulusan Volcano, a resurgent volcano.

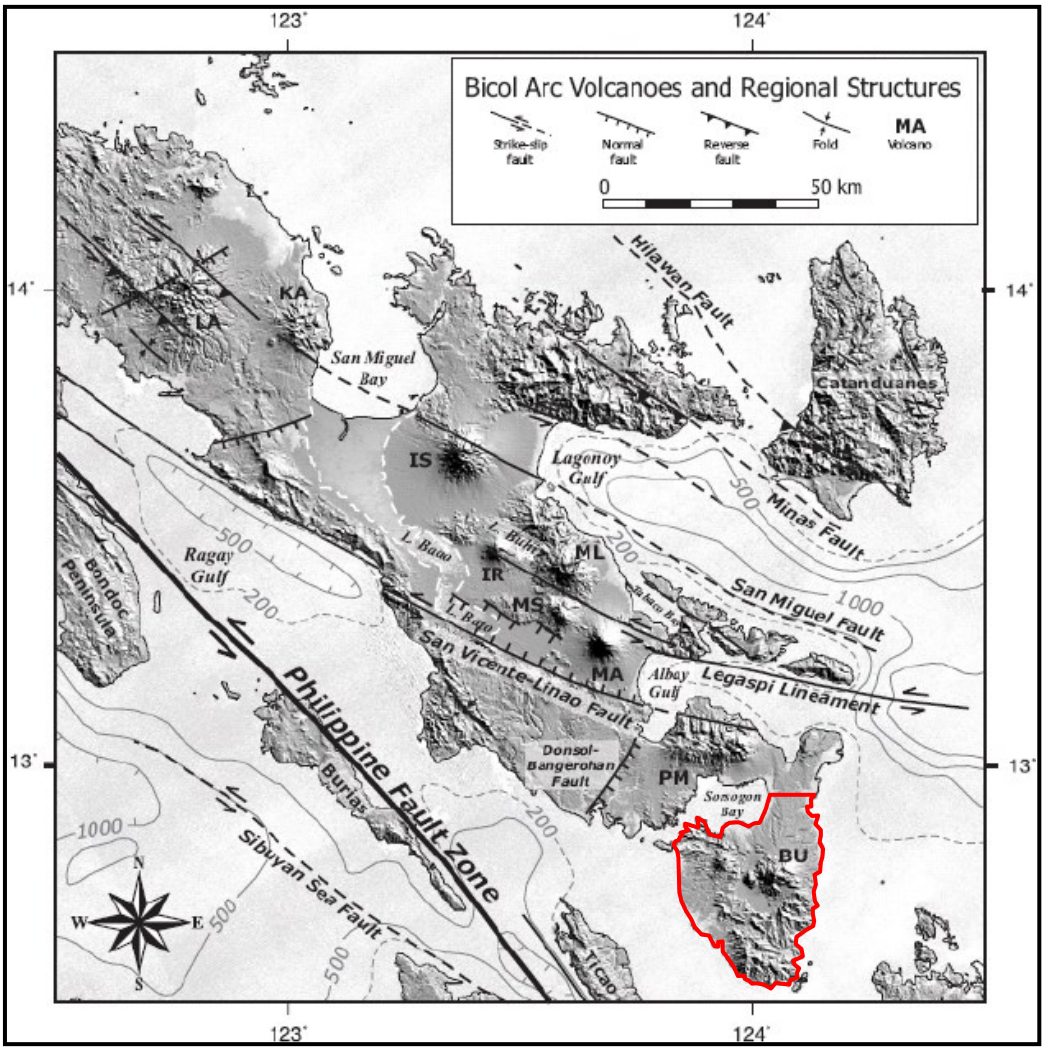

Figure 1: The most prominent structures near the study area trend northwest-southeast (i.e., San Miguel Fault, Legaspi Lineament, and San Vicente-Linao Fault), representing the major tectonic grain of the Bicol Volcanic Arc. The absence of delineated structures within the Bulusan Volcanic Complex, outlined in red, at the southernmost tip of the arc is evident in this map. Figure is taken from Tengonciang (2008).

3. METHODOLOGY

Topographic models, in particular shaded relief and slope aspect maps, were generated for the Bulusan Volcanic Complex to facilitate the initial interpretation of structures, providing a picture of the general tectonic grain, as well as the location of structures and their orientation. The wide coverage of remotely-sensed imagery offers a synoptic view, ideal for interpreting large-scale structures characteristic of tectonically-deformed regions.

From the topographic models, two prominent WNW-ESE-trending large-scale lineaments were identified to border the northern and southern rim of the Irosin caldera (Figure 2). Two GPR survey lines were conducted across the inferred trace of the southern lineament, namely the Bagsangan and Gabao lines. The Bagsangan GPR line (Figure 2) was strategically positioned to traverse the central segment of the southern lineament to determine whether it is continuous. This GPR line scan is almost straight and trends N20^{o}E. The Gabao transect survey (Figure 2) is a curved line with a general trend of N25^{o}W. Halfway through the transect, the direction shifts to N60^{o}W because of the road direction. The start and end positions of each of these surveys were mapped using a Global Positioning System (GPS).

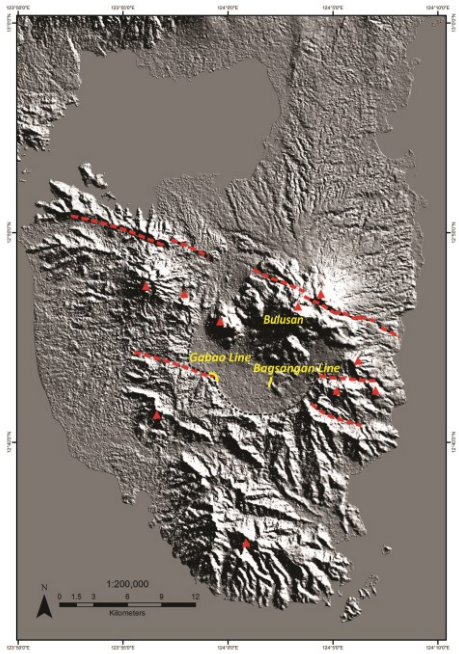

Figure 2: Map showing the actual trace of the GPR scan lines (yellow) in Irosin caldera. The red dotted lines represent the northern and southern lineament that borders the Irosin caldera. The black dotted line is the trace of the Irosin caldera. Red triangles are the volcanic centers within the Bulusan Volcanic Complex.

4. RESULTS

The lineament maps produced from shaded relief and slope aspect maps showed large-scale structures found within the study area. These maps served as target areas for the conduct of GPR survey.

4.1 Shaded Relief Images

Shaded relief imageries (Figures 3-6) revealed several sets of lineament structures that dissect the entire Bulusan Volcanic Complex. Most of these lineaments, particularly the large-scale ones, were consistently identifiable in all the generated models. However, depending on the sun azimuth, some lineaments appeared subdued and/or washed out.

4.1.1 WNW-ESE Lineaments

The most prominent structures observed in all of the generated shaded relief images were the northern and southern lineaments that border the northern and southern rims of the Irosin caldera. The northern lineament was defined by the shadow of a linear ridge about 12 km-long and striking about N60^{o}W. The trace of the ridge extended towards Bulusan volcano to the east, where its appearance becomes subdued probably because of persistent deposition of more recent volcanic materials. Parallel to the northern lineament, towards the south, a WNW-ESE alignment of volcanoes and volcanic cones was evident. The physical location of the active Bulusan volcano appeared to be along the intersection of the northern lineament with a NNW-SSE striking structure. The southern lineament, on the other hand, was defined by a deeply dissected gully to the southwest and a linear caldera rim to the southeast. This structure appeared to be a single and continuous lineament with a missing central segment.

Numerous WNW-ESE lineaments were also traced towards the south of the Irosin caldera. These lineaments were generally represented by deeply incised linear valleys. Particularly notable is Mt. Calungalan, an elongate and offset volcano southwest of the caldera. This volcano is truncated by intersecting WNW-ESE and NNW-SSE trending lineaments. The offset seen in Mt. Calungalan suggests a left-lateral sense of movement for WNW-ESE lineament and a right-lateral sense of movement for the NNW-SSE lineament (Figure 7).

4.1.2 NNW-SSE Lineaments

Three prominent and large-scale NNW-SSE- trending lineaments were observed in the eastern and western portions of the study area. These were represented by deeply incised linear valleys cutting through Mts. Bulusan, Bintacan and Calungalan. NNW-SSE-trending lineaments that traverse Mt. Bulusan was cut by the northern lineament (WNW-ESE trend). In the western portion of the area, these NNW-SSE- trending lineaments appear to have influenced instability of Mt. Bintacan that led to its collapse as well as the elongated outline of Mt. Calungalan.

4.1.2 NE-SW Lineaments

In some of the shaded relief models, NE-SW lineaments were also evident but not pervasive. They were particularly visible when the illumination was perpendicular to its strike, either from 135^{o} or 315^{o} azimuth. These structures were represented by relatively linear ridges and mostly concentrated in the western part of the area.

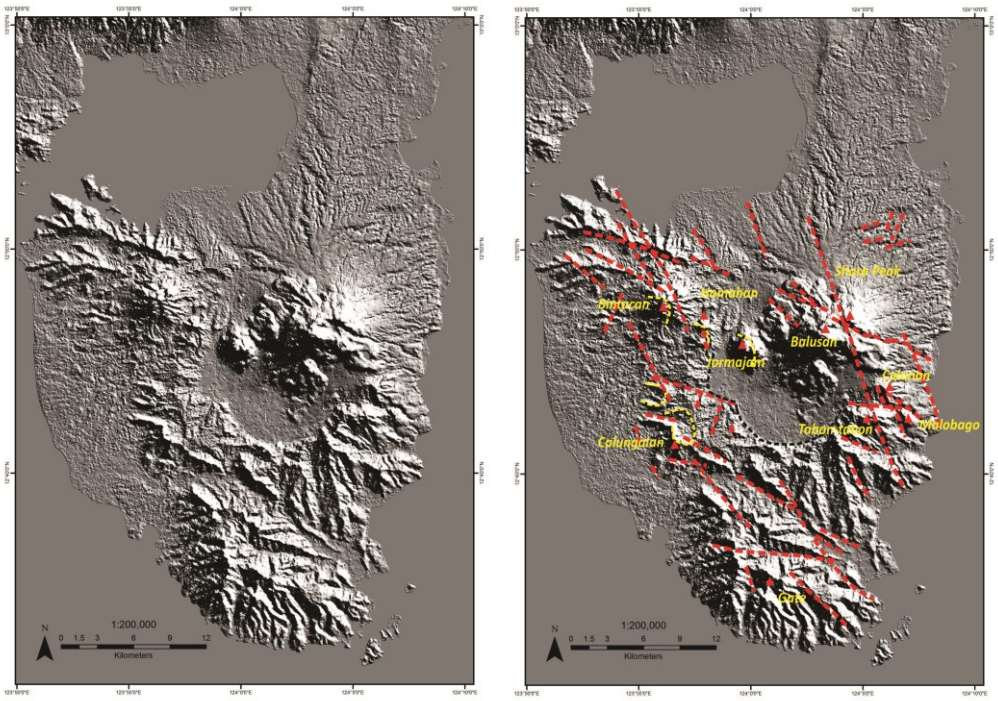

Figure 3: SAR DSM shaded relief of the Irosin caldera, sun elevation at 45^{o} and azimuth at 45^{o}. Red dashed lines represent lineament traces. Black dashed line outlines the caldera. Yellow dashed lines are collapsed features and offset volcanic crater.

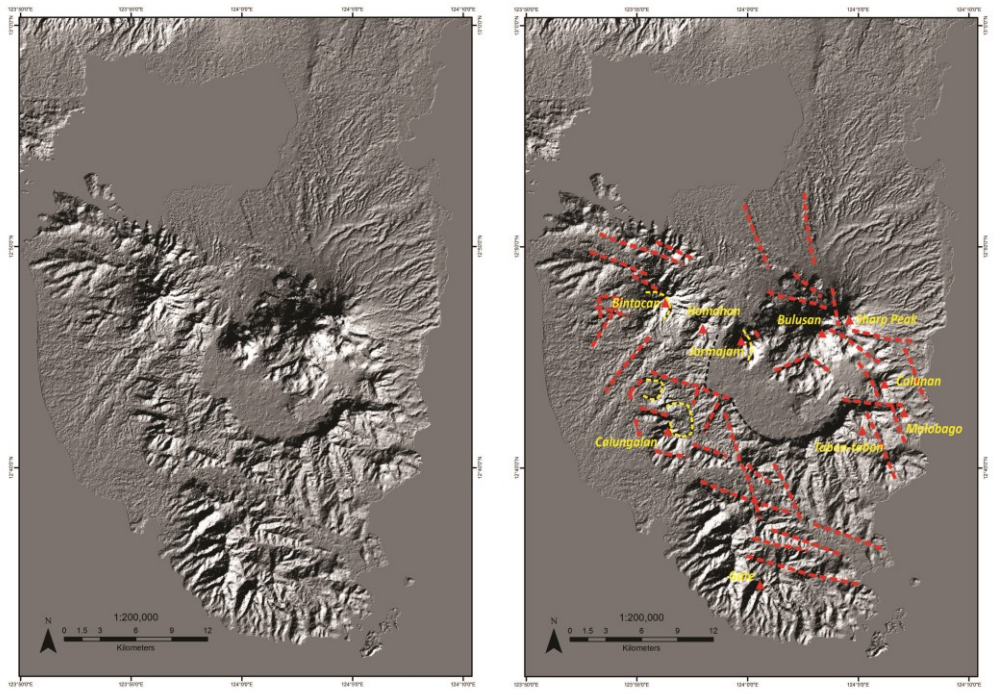

Figure 4: SAR DSM shaded relief of the Irosin caldera, sun elevation at 45^{o} and azimuth at 135^{o}. Red dashed lines represent lineament traces. Black dashed line outlines the caldera. Yellow dashed lines are collapsed features and offset volcanic crater.

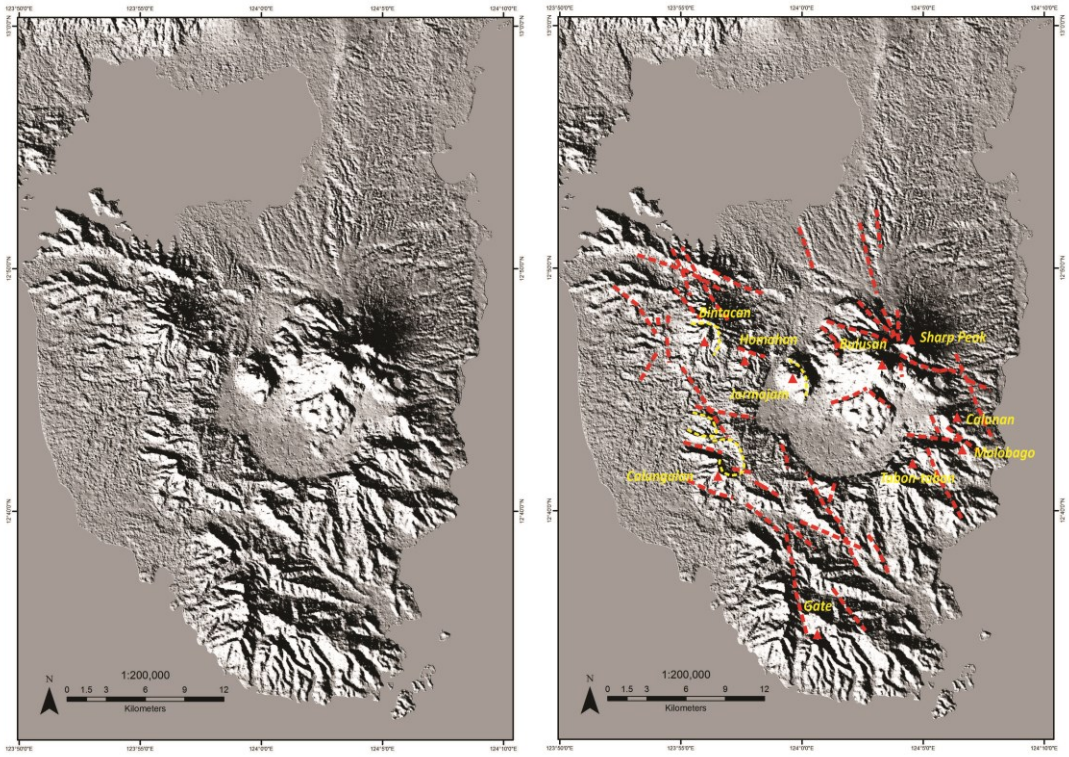

Figure 5: SAR DSM shaded relief of the Irosin caldera, sun elevation at 45^{o} and azimuth at 225^{o}. Red dashed lines represent lineament traces. Black dashed line outlines the caldera. Yellow dashed lines are collapsed features and offset volcanic crater.

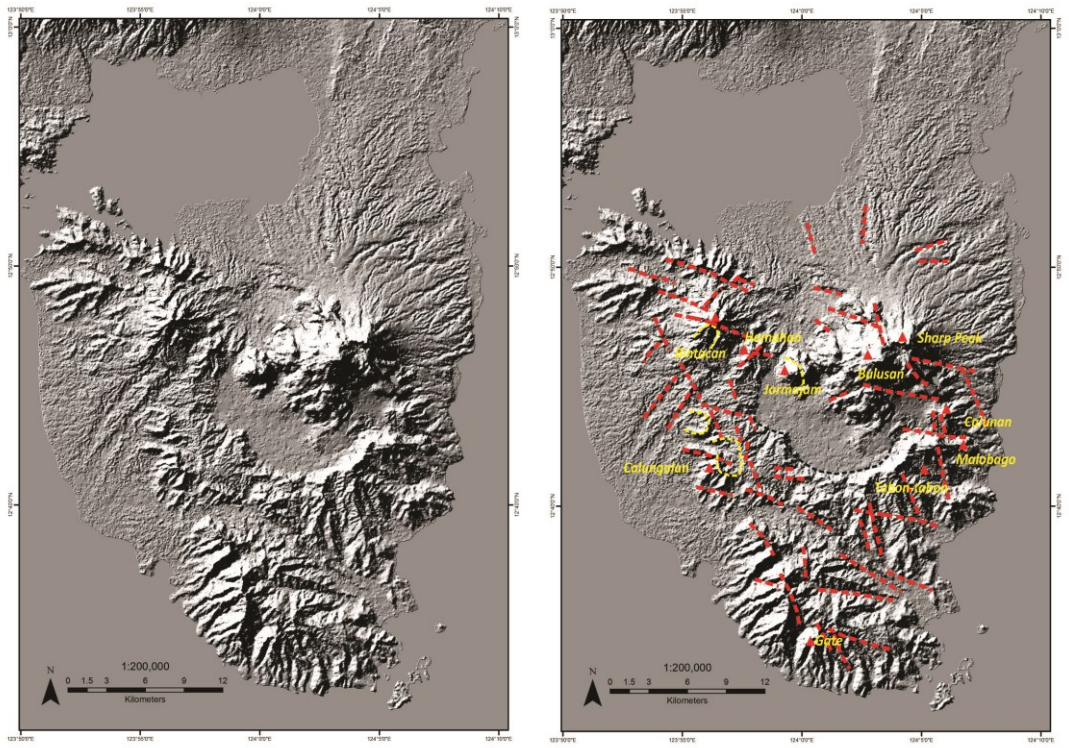

Figure 6: SAR DSM shaded relief of the Irosin caldera, sun elevation at 45^{o} and azimuth at 315^{o}. Red dashed lines represent lineament traces. Black dashed line outlines the caldera. Yellow dashed lines are collapsed features and offset volcanic crater.

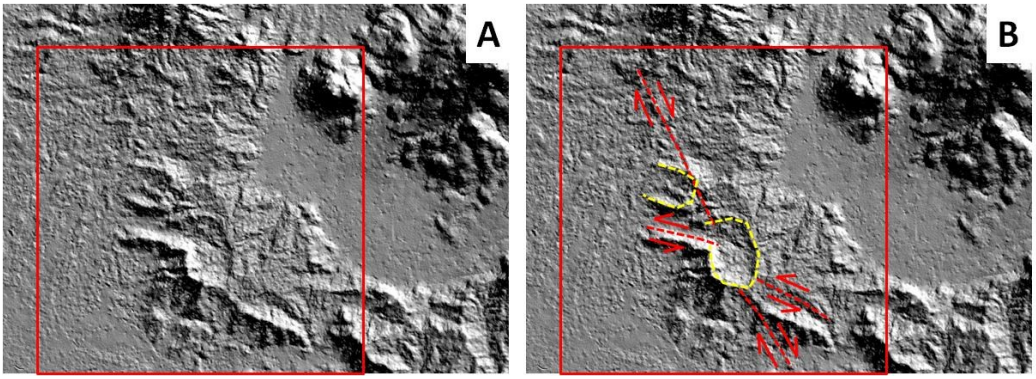

Figure 7: Based on elongate and offset volcanic center and displaced lineament, a left-lateral sense of movement can be inferred for the WNW-ESE and a right lateral sense of movement for the NNW-SSE-trending structures.

4.2 Slope Aspect Maps

Consistent with that of the shaded relief models, slope aspect maps also show three distinct uniform slope patterns, which correspond to the WNW-ESE-, NNW-SSE- and NE-SW- trending lineaments (Figure 8). In the grayscale map, the most pronounced pattern based on uniform aspect was the WNW-ESE trend (yellow arrows). Both the northern and southern lineaments bounding the Irosin caldera were also identified in the models. The northern lineament was observed to dip towards the south while the southern lineament towards the north. Similarly, the colored aspect map highlighted the WNW-ESE trending structures (marked by black arrows) that border the northern and southern rims of the Irosin caldera as well as those that dissect the southern portion of the study area. Towards the east, NE-SW-trending lineaments (marked by pink and gray arrows) consistently appeared in both aspect maps. The NNW-SSE-lineaments (red and white arrows) were also observed but not as clearly defined.

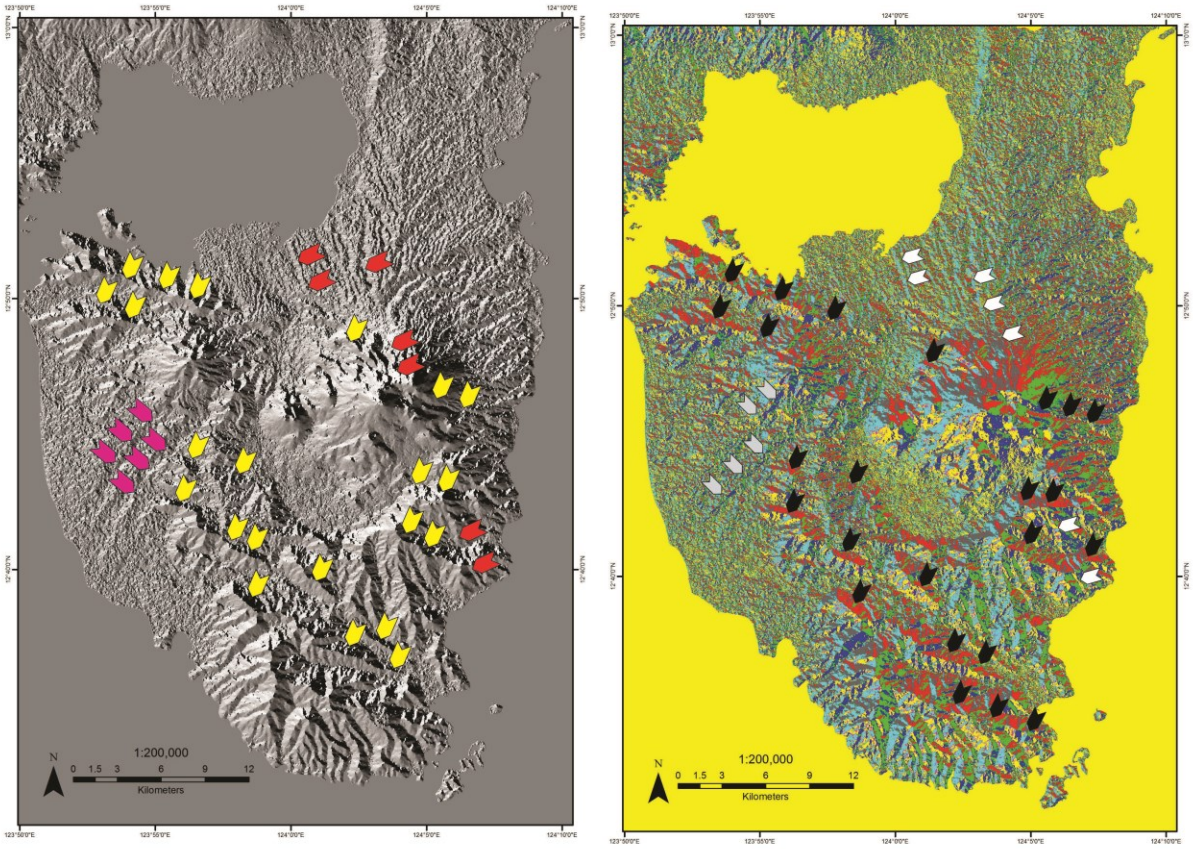

Figure 8: Gray-scale and colored RGB slope aspect images of the Bulusan Volcanic Complex. Arrows point to uniform slopes and planar surfaces. (Left: Grayscale) yellow – NW-SE trend; red – NNW-SSE trend; pink – NE-SW. (Right: Colored RGB) black – NW-SE trend; white – NNW-SSE trend; gray – NE-SW trend.

4.3 Ground Penetrating Radar

Figures below represent the processed GPR data along lines of Bagsangan and Gabao. These scan lines have a total horizontal length of about 810 m and 1,450 m, respectively. GPR profiles generated from scan line Bagsangan crossed the central segment of

the southern lineament while those produced from scan line Gabao crossed the southern lineament along the southwestern margin of the caldera. The GPR profiles show a variety of discontinuities within the upper 10 m of the subsurface, which correspond to the maximum depth of penetration attained in this survey.

GPR profiles Bagsangan 1 to Bagsangan 11 (Figures 9-12) are segments of the Bagsangan transect line. These scans are supposed to be continuous; however, a minor equipment interruption encountered during the survey necessitated a restart of the GPR instrument. Figures 13-15 represent the scan lines for Gabao.

4.3.1 Bagsangan Traverse

The first 200 m of the Bagsangan traverse is uniform without any major structural feature observed (Figure 9). Most of the reflectors are relatively horizontal and undisturbed. The next 300 m of the GPR traverse, however, showed several reflectors that are steeply dipping NW-SE-trending normal faults and a few inclined 60-70^{o} faults (Figure 10). Most of the identified faults and fractures affect more than 7-8 m thickness of the underlying deposit. The faults defined along Bagsangan 7 segment correspond to the inferred trace of the central segment of the southern lineament (Figure 11). This segment revealed a series of NW-SE-trending graben-like structures with dips of about 60-70^{o}. The next 170 m of the traverse are relatively undisturbed reflectors of the shallow subsurface. However, towards the north-northeastern end of the profile (Bagsangan 11), a major graben-like structure is significantly noticeable. Similar with the other graben-features, this major fault is NW-SE-trending and has a relatively steep dip of about 70^{o} (Figure 12).

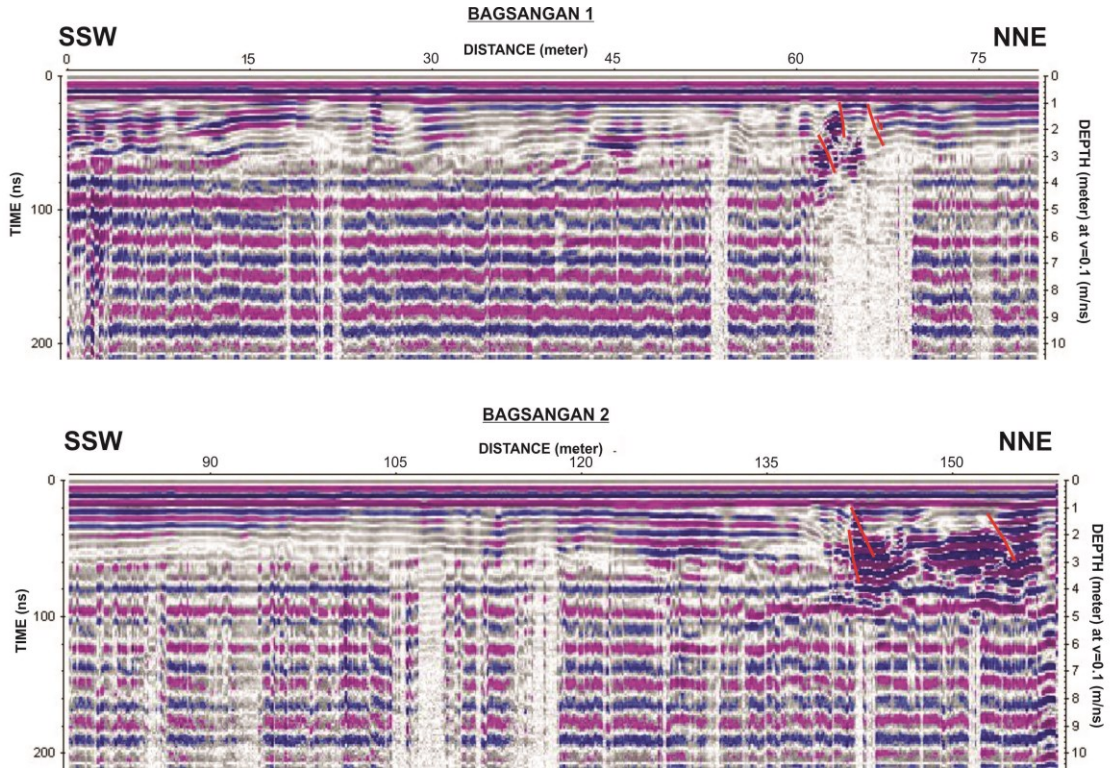

Figure 9: GPR Profiles Bagsangan 1 and 2 represent the first ~150 m of the Bagsangan transect. Red lines point to trace of faults and fractures based on deflected radar signals.

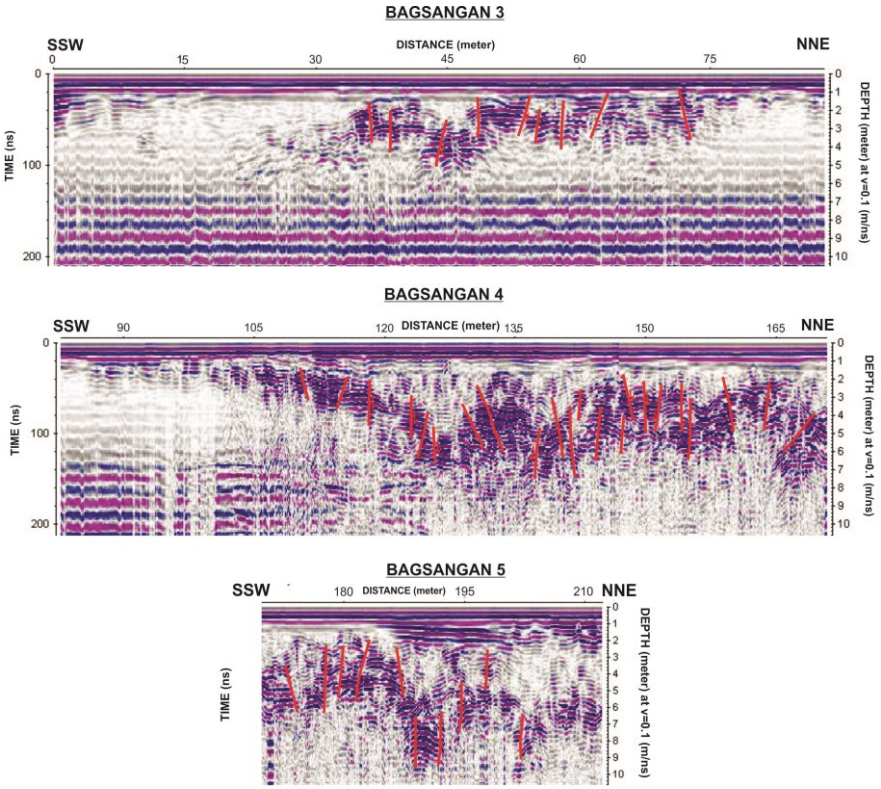

Figure 10: GPR Profiles Bagsangan 3-5 represent the next ~210 m of the Bagsangan transect. Red lines point to trace of faults and fractures based on deflected radar signals.

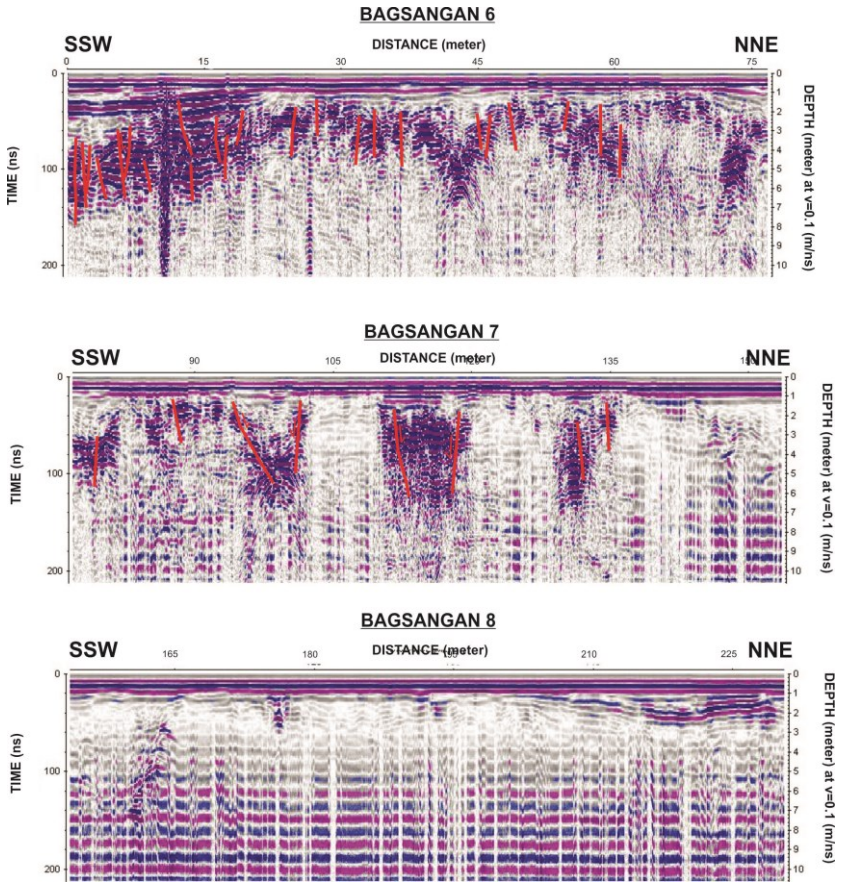

Figure 11: GPR Profiles Bagsangan 6-8 represent the next ~230 m of the Bagsangan transect. Red lines point to trace of faults and fractures based on deflected radar signals. Bagsangan 7 profile corresponds to the inferred trace of the southern lineament.

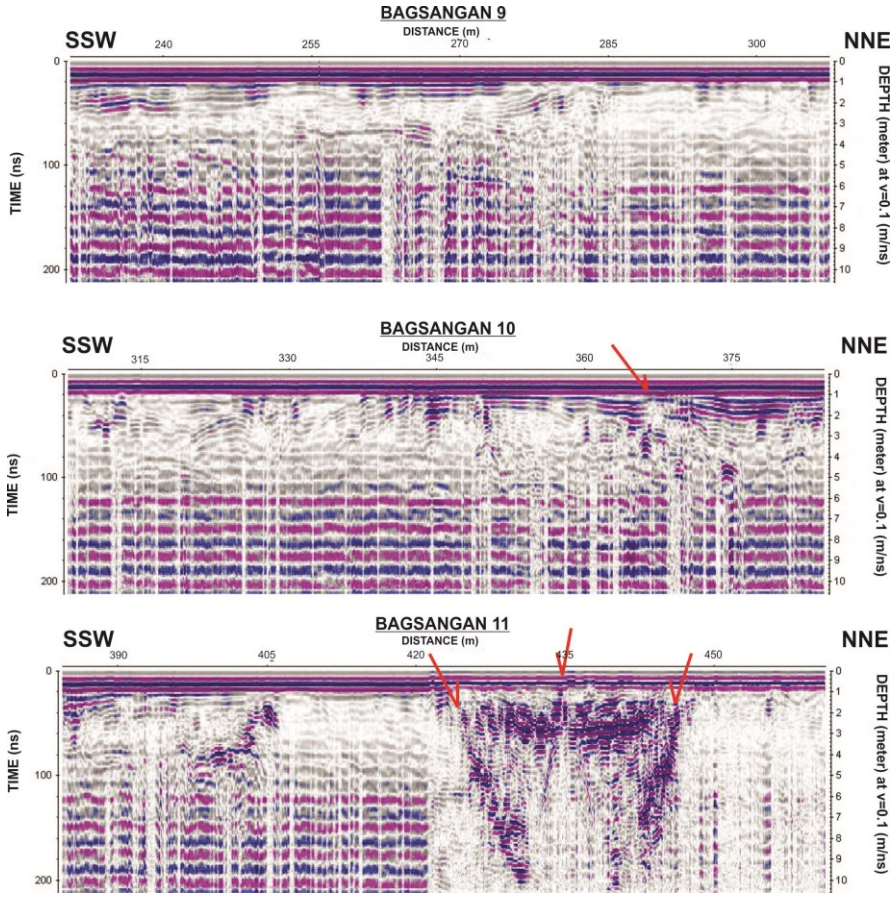

Figure 12: GPR Profiles Bagsangan 9-11 represent the last ~230 m of the Bagsangan transect. Red lines point to trace of faults and fractures based on deflected radar signals.

4.3.2 Gabao Traverse

Profiles Gabao 1-8 (Figures 13-15) represent the processed GPR data from Gabao line. The first 560m of the traverse was relatively undisturbed with only minor steeply dipping offset reflectors which exhibit normal fault movement at 240-260 m, 425 m and 510 m lateral distance (Figure 13). The GPR reflections from 650-750 m laterally (Profile Gabao 4) correspond to the inferred trace of the southern lineament. Several parallel NW-SE-trending faults with normal fault displacements are seen in the GPR profiles. Since the trace is almost vertical, it is possible that there is a lateral component associated with these faults but not seen in the GPR sections. Up to 750 m horizontal distance, the GPR scan was following a SE-NW trend aimed to go across the trace of the southern lineament. However, starting at 760 m horizontal distance, the Gabao transect shifted course from SE-NW to ESE-WNW. At this point, the Gabao traverse did not go across the lineament but instead ran parallel to the inferred plane of the southern lineament. Nevertheless, numerous steeply dipping offset reflectors which indicate normal fault movement were still observed up to the end of the traverse at 1450 m distance. These faults and fractures may be correlated to the NE-SW-trending linear features towards the southwestern margin of the caldera. In general, reflectors in the Gabao traverse were only traceable to a depth of about 9 m.

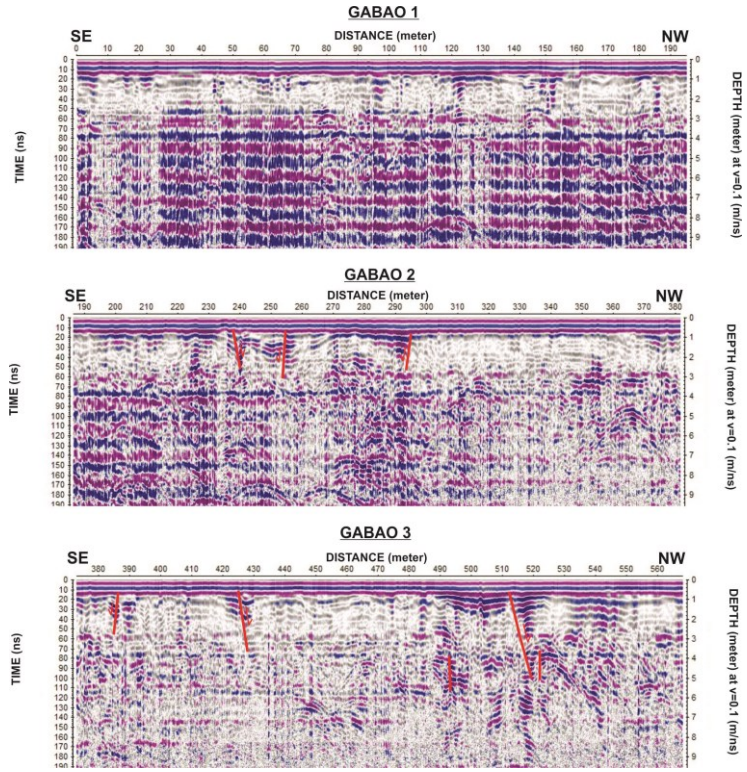

Figure 13: GPR Profiles Gabao 1-3 represent the first 560 m of the Gabao transect. Red lines point to trace of faults and fractures based on deflected radar signals

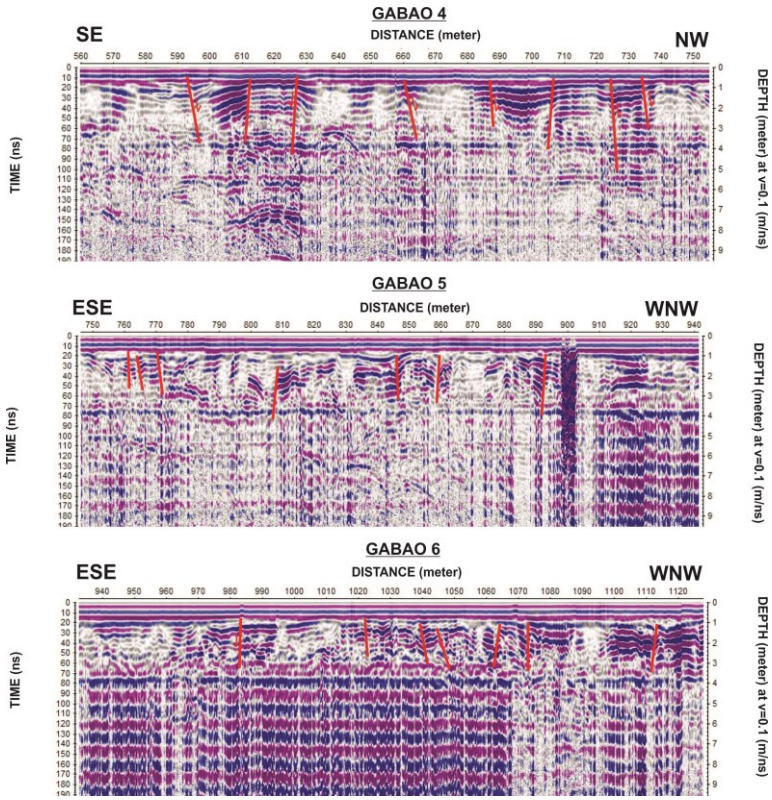

Figure 14: GPR Profiles Gabao 4-6 represent the next 560 m of the Gabao transect. Red lines point to trace of faults and fractures based on deflected radar signals. Gabao 4 profile corresponds to the inferred trace of the southern lineament.

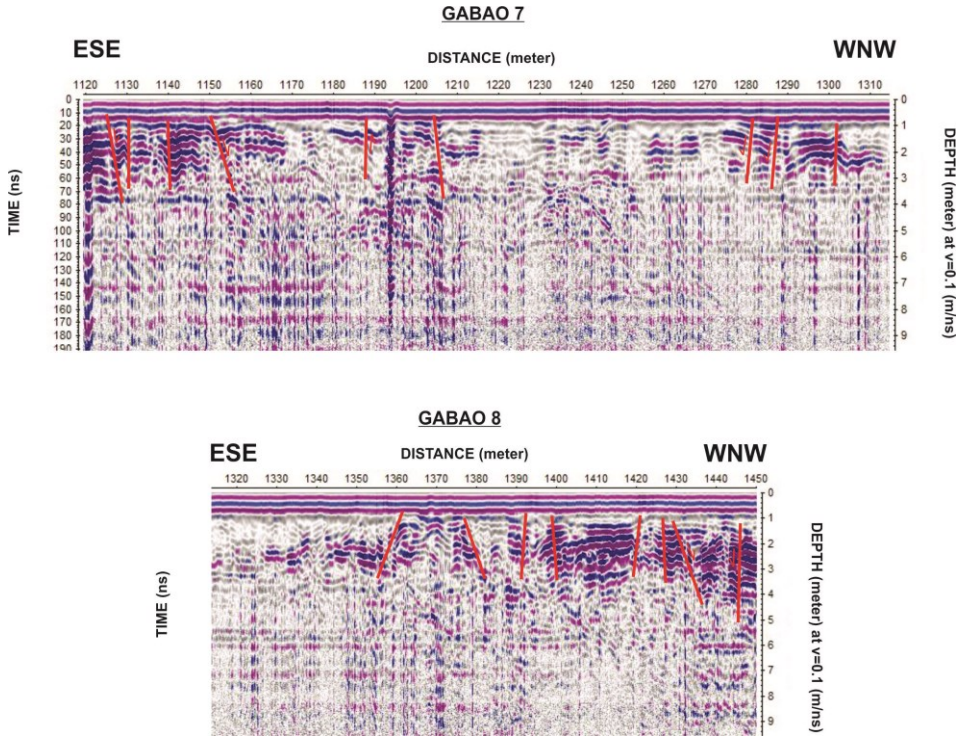

Figure 15: GPR Profiles Gabao 7-8 represent the last 330 m of the Gabao transect. Red lines point to trace of faults and fractures based on deflected radar signals.

5. DISCUSSIONS AND CONCLUSION

The shaded relief and slope aspect models provided a better view of the structures present within the Irosin caldera and surrounding areas. These topographic models clearly outlined relevant morphological units, such as slope, texture, collapse, linear and offset features, giving important insights into the possible relationship between regional tectonics and volcanoes within the study area. Active regional tectonic settings dominated by strike-slip fault systems are typically characterized by aligned volcanoes and volcanic cones, elongated basins, lakes and pull-apart grabens (Aydin and Nur, 1982; Sylvester, 1988). All of these features, except for the lake, are present in the Irosin study area and it would appear that the Irosin caldera itself is consistent with a pull-apart structure. This is not the first case wherein pull-apart structures have been associated with calderas. The evolution of Tondano caldera in Indonesia was attributed to the formation of a pull-apart basin in a releasing stepover ENE-WSW sinistral fault zone (Lecuyer et al., 1997)

The Irosin caldera exhibits a non-circular shape and is partly bounded on its northern and southern margins by WNW-ESE lineaments. Along with the presence of aligned volcanoes and volcanic cones in the area, one is led to hypothesize that the region has been deformed by fault movement. Based on earlier studies, calderas that deviate from the conventional circular or semi-circular shape are generally tectonically-formed (Bellier and Sébrier, 1994; Lecuyer et al., 1997). The WNW-ESE- trending set of faults and fractures are probably responsible for the elongate and polygonal shape of the Irosin caldera.

In general, the GPR survey provided interpretable images of shallow subsurface structures beneath the Irosin caldera floor. Several faults and fractures were recognized on the reflection profiles based on the lateral continuity, thickness variations, changes in dip angle and orientation of reflectors, and displacement of reflectors, as previously stated. However, due to signal degradation at depth, faults and fractures cannot be identified past 10 m but most likely extend deeper. Structures that propagate more than 7-8 m thickness of the underlying deposit are considered major for this study. Most of the faults and fractures traced in both Gabao and Bagsangan transects are steeply-dipping and display vertical displacements. Both normal and reverse faults were recognized based on vertical displacements that abruptly terminated reflectors. However, steeply-dipping normal faults were more abundant and may be interpreted as oblique-slip faults.

The lineament and GPR interpretations of the WNW-ESE structures that bound the Irosin caldera are consistent with the current understanding of the recognized tectonic structures that splay from the Philippine Fault towards the Bicol Peninsula. Hence, it can be deduced that the stress regime acting on the entire Peninsula is consistent. In relation to the ongoing geothermal exploration in the area, these identified structures may serve as general pathways of fluid to the surface.

REFERENCES

Acocella, V., Salvini, F., Funiciello, R. and Faccenna, C.: The Role of Transfer Structures on Volcanic Activity at Campi Fleigrei (Southern Italy), *Journal of Volcanology and Geothermal Research*, **91** (1999), 123-139.

Aydin, A. and Nur, A.: Evolution of Pull-Apart Basins and their Scale Independence, *Tectonics*, **1** (1982), 91-105.

Bellier, O. and Sébrier, M.: Relationship Between Tectonism and Volcanism along the Great Sumatran Fault Zone Deduced by Spot Image Analyses, *Tectonophysics*, **233** (1994), 215-231.

Delfin, F.G.: Petrogenesis of Mt. Bulusan Volcanic Complex, Bicol Arc, Philippines, *Master's Thesis*, University of South Florida (1991).

Delfin, F.G., Panem, C.C. and Defant, M.J.: Eruptive History and Petrochemistry of the Bulusan Volcanic Complex: Implications for the Hydrothermal System and Volcanic Hazards of Mt. Bulusan, Philippines, *Geothermics*, **22** (1993), 417-434.

Holohan, E.P., Troll, V.R., Walter, T.R., Munn, S., McDonnell, S. and Shipton, Z.K.: Elliptical Calderas in Active Tectonic Settings: An Experimental Approach, *Journal of Volcanology and Geothermal Research*, **144** (2005), 119-136.

Holohan, E.P., van Wyk de Vries, B. and Troll, V.R.: Analogue Models of Caldera Collapse in Strike Slip Tectonic Regimes, *Bulletin of Volcanology*, **70** (2008), 773-796.

Lagmay, A.M.F., Tengonciang, A.M.P. and Uy, H.S.: Structural Setting of the Bicol Basin and Kinematic Analysis of Fractures on Mayon Volcano, Philippines, *Journal of Volcanology and Geothermal Research*, **144** (2005), 23-36.

Lecuyer, F., Bellier, O., Gourgaud, A. and Vincent, P.M.: Active Tectonics of the North-east Sulawesi (Indonesia) and the Structural Control of the Tondano Caldera, *C.R. Acad. Sci., Paris*, **325** (1997), 607-613.

Mirabueno, M.H.T., Okuno, M., Nakamura, T., Laguerta, E.P., Newhall, C.G. and Kobayashi, T.: AMS Radiocarbon Dating of Charcoal Fragment from the Irosin Ignimbrite, Sorsogon Province, Southeastern Luzon, Philippines, *Bulletin of Volcanological Society of Japan*, **52** (2007), 241-244.

Pasquare, F.A. and Tibaldi, A.: Do Transcurrent Faults Guide Volcano Growth? The Case of NW Bicol Volcanic Arc, Luzon, Philippines, *Terra Nova*, **15** (2003), 204-212.

Sanderson, D.J. and Marchini, W.R.D.: Transpression, *Journal of Structural Geology*, **6** (1984), 449-458.

Sylvester, A.G.: Strike-slip Faults, *Geological Society of America Bulletin*, **100** (1988), 1666-1703.

Tengonciang, A.M.P.: Tectonic deformation of Mayon Volcano, Philippines, *Master's Thesis*, University of the Philippines, Diliman, Quezon City, (2008).